Regenerative Therapy and Cancer: *In Vitro* and *In Vivo* Studies of the Interaction Between Adipose-Derived Stem Cells and Breast Cancer Cells from Clinical Isolates

Ludovic Zimmerlin, Ph.D.,[1,2] Albert D. Donnenberg, Ph.D.,[1–3] J. Peter Rubin, M.D.,[3,4]
Per Basse, M.D., Ph.D.,[1] Rodney J. Landreneau, M.D.,[4,5] and Vera S. Donnenberg, Ph.D., F.C.P.[1,3–5]

Adipose-derived stem cells (ASCs) have been proposed to stabilize autologous fat grafts for regenerative therapy, but their safety is unknown in the setting of reconstructive surgery after mastectomy. Both bone marrow mesenchymal stem cells (MSCs) and ASC have been shown to enhance tumorigenesis of established breast cancer cell lines, but primary patient material has not been tested. Here, we ask whether ASC promote the *in vitro* growth and *in vivo* tumorigenesis of metastatic breast cancer clinical isolates. Metastatic pleural effusion (MPE) cells were used for coculture experiments. ASC enhanced the proliferation of MPE cells *in vitro* (5.1-fold). For xenograft experiments (100 sorted cells/injection site), nonhematopoietic MPE cells were sorted into resting and active populations: CD90+ resting (low scatter, 2.1% ≥2N DNA), CD90+ active (high scatter, 10.6% ≥2N DNA), and CD90−. Resting CD90+ MPE cells were tumorigenic in 4/40 sites but growth was not augmented by ASC. Active CD90+ MPE cells were tumorigenic (17/40 sites) only when coinjected with ASC ($p = 0.0005$, χ^2 test). The multilineage potentiality and MSC-like immunophenotype of ASC were confirmed by flow cytometry, differentiation cultures, and immunostaining. The secretome profile of ASC resembled that reported for MSC, but included adipose-associated adipsin and the hormone leptin, shown to promote breast cancer growth. Our data indicate that ASC enhance the growth of active, but not resting tumor cells. Thus, reconstructive therapy utilizing ASC-augmented whole fat should be postponed until there is no evidence of active disease.

Introduction

AUTOLOGOUS FAT TRANSFER for soft tissue reconstruction was initially described more than a century ago for correction of facial defects[1] and was soon after introduced for breast reconstruction postmastectomy.[2] However, fat injection into the breast became controversial among plastic surgeons because of potential complications such as local calcifications and interference with mammographic breast cancer surveillance.[3] Autologous fat transfer remains an attractive reconstructive technique with low complication rates,[4] but variability in long-term graft survival[5,6] has been attributed to differences in local angiogenesis.[7,8] Recently, the addition of adipose-derived stem cells (ASCs) to whole fat grafts was proposed to support the formation of a new vasculature[9,10] and promote graft retention.[11] Fat tissue is a rich source of both endothelial progenitors[12,13] and multipotent mesenchymal stem cells (MSCs), which when ex-

panded in short-term culture have been termed ASC.[14–16] ASC phenotypically resemble bone marrow (BM) MSCs[14] and share their multipotentiality,[15] but are far more prevalent in fat than BM-MSC are in bone marrow aspirates. While ASC and BM-MSC are promising candidates for reconstructive cellular therapy postmastectomy, the potential risk of promoting tumor reactivation is controversial. This is especially germane considering that up to 20% of breast cancer patients will suffer from cancer recurrence during the first decade after adjuvant therapy.[17] In this article, human breast cancer cells were characterized from freshly isolated pleural fluids.[18,19] We developed an *in vitro* coculture system to measure their recruitment by shortly expanded human ASC, as compared to BM-MSC. For xenograft studies, nonhematopoietic, nonendothelial MPE tumor cells were sorted into low light scatter CD90+, high light scatter CD90+, and CD90− fractions, and were coinjected (100 cells/site) with ASC into the mammary fat pads of immunodeficient mice.

[1]University of Pittsburgh Cancer Institute, Pittsburgh, Pennsylvania.
[2]Division of Hematology/Oncology, Department of Medicine, University of Pittsburgh School of Medicine, Pittsburgh, Pennsylvania.
[3]McGowan Institute of Regenerative Medicine, Pittsburgh, Pennsylvania.
[4]Department of Surgery, University of Pittsburgh School of Medicine, Pittsburgh, Pennsylvania.
[5]Heart Lung and Esophageal Surgery Institute, Pittsburgh, Pennsylvania.

Methods

Fat tissue collection, stromal vascular fraction isolation, and ASC preparation

Subcutaneous adipose tissue was harvested during abdominoplasty from human adult male and female patients at Magee Womens Hospital, Pittsburgh, PA. All samples were waste materials collected as a byproduct of surgery. De-identified samples were collected under an IRB-approved exemption (number 0511186, University of Pittsburgh IRB). Upon reception in the laboratory, fat tissue was processed directly for isolation of stromal vascular fraction (SVF), as previously described.[20] Fat tissue was minced; digested for 30 min in Hanks' balanced salt solution (HBSS; Invitrogen), 3.5% bovine serum albumin (BSA; Millipore), and 1 mg/mL collagenase type II (Worthington) on a shaking water bath at 37°C; and disaggregated through successive 425 μm and 180 μm sieves (W.S. Tyler). After elimination of mature adipocytes by centrifugation (400 g, ambient temperature, 10 min) and red blood cell lysis (NH$_4$Cl-based buffer [Beckman-Coulter, Cat No. IM3630d], ambient temperature, 10 min), cells were washed in phosphate-buffered saline (PBS) and mononuclear SVF cells were enriched on a Ficoll-Hypaque density gradient (Histopaque®-1077; Sigma-Aldrich). ASC were selected by adherence after plating SVF at a density of 10–20,000 cells/cm^2 in proliferation culture medium (PCM, DMEM, and DMEM/F12, 1:2, 10% fetal bovine serum [FBS] and 0.1μM dexamethasone [Sigma]) in uncoated T75 or T150 flasks (BD Biosciences Falcon).

Flow cytometric staining of ASC

Harvested ASC were maintained on ice and stained for analytical flow cytometry as previously described.[18,21] Cell suspensions were centrifuged (200 g, 7 min) and the cell pellet was preincubated with 5 μL neat mouse serum (Sigma) to minimize nonspecific antibody binding. Cells were simultaneously stained with monoclonal mouse anti-human fluorochrome-conjugated antibodies (2 μL each, tube 1: CD3-fluorescein isothiocyanate [FITC; IM1281], CD146-phycoerythrin [PE; A07483], CD34-energy coupled dye [ECD; IM2709U], CD90-PE-Cy5 [IM3703], and CD117-PE-Cy7 [IM3698] [all from Beckman-Coulter], CD31-allophycocyanin [APC; FAB3567A; R&D Systems], and CD45-APC-Cy7 [BD Biosciences, 348805], and tube 2: CD105-FITC [Fitzgerald Industries 61R-CD105dHUFT], CD73-PE [BD Pharmingen 550257], CD34-ECD, CD90-APC [BD Pharmingen 559869], and CD44-PE-Cy7 [Abcam ab46793], and CD45-APC-Cy7). Stained samples were washed in PBS, 0.1% sodium azide, 4% calf serum, fixed with 2% methanol-free formaldehyde (Polysciences, Inc.), permeabilized in PBS with 0.1% saponin (Coulter), 0.5% BSA for 10 min at ambient temperature, and incubated with 7.7 μg/mL 4′,6-diamidino-2-phenylindole (DAPI; Invitrogen). Eight-color, 14-parameter data files were acquired on a three-laser CyAn ADP cytometer (Beckman-Coulter). Up to 10,000,000 events were acquired per sample without exceeding an acquisition rate of 10,000 events/second. For fixed permeabilized samples, DAPI fluorescence was captured by 2 individual photomultiplier tubes that were optimized for logarithmic (elimination of hypodiploid events) and linear (cell cycle analysis) scales, respectively. Offline compensation and analysis were performed using high-throughput parallel processing VenturiOne software (Applied Cytometry). The compensation matrix was created based on the acquisition of BD Calibrite™ beads (FITC, PE, and APC; BD Biosciences) and single antibody-stained mouse IgG capture beads (552843; BD Biosciences) for tandem-dyes (ECD, PE-Cy5, PE-Cy7, and APC-Cy7). Five independent samples were analyzed. Flow cytometric results were summarized as arithmetic means ± standard deviation (SD) and ± standard error of the mean (SEM), to convey both sample to sample variability (SD) and the precision of the mean values (SEM).[22]

Carboxyfluorescein succinimidyl ester-labeling of ASC

Low-passage ASC were trypsinized and transferred into polypropylene tubes. Cells were washed twice in PBS and incubated for 15 min at 37°C in prewarmed 5μM 5-(and 6-)-carboxyfluorescein diacetate succinimidyl ester (CFDA-SE, C-1157; Invitrogen) solution in PBS. Cells were washed and then incubated for 30 min at 37°C in the prewarmed culture medium (PWCM) to allow complete acetate hydrolysis of CFDA-SE into carboxyfluorescein succinimidyl ester (CFSE). Cells were washed in the culture medium and counted on a hemacytometer using Trypan blue to assess cell viability.

ASC differentiation: Adipogenesis, osteogenesis, and chondrogenesis

Low-passage ASC (≤P3) were trypsinized and split for concomitant differentiation toward all 3 lineages. For adipogenesis and osteogenesis, ASC were transferred to tissue culture-treated plastic 6-well plates (BD Falcon 353046) at 25,000 cells/cm^2 and allowed to adhere overnight in PCM. The next day, the culture medium was supplemented for lineage-specific differentiation. Adipogenic cultures contained 1 μM dexamethasone (D2915; Sigma-Aldrich), 0.5 μM isobutylmethylxantine (I5879; Sigma-Aldrich), 60 μM indomethacin (I7378; Sigma-Aldrich), and 10μg/mL insulin (I2643; Sigma-Aldrich). Osteogenic cultures contained 0.1 μM dexamethasone, 50 μg/mL L-Ascorbic acid (A8960; Sigma-Aldrich), and 10 mM beta-glycerolphosphate (G9891; Sigma-Aldrich). ASC were allowed to differentiate for 21 days before fixation in PBS and 2% formaldehyde (Polysciences, Inc., 15 min, room temperature). To assess adipogenic differentiation, fixed cells were washed in 60% isopropanol and stained for 10 min with Oil Red O (O0625; Sigma-Aldrich). After osteogenic differentiation, alkaline phophatase (ALP) activity was revealed using the ALP leukocyte kit (86C-1KT; Sigma-Aldrich). Alternatively, fixed cells were washed in PBS and stained for 10 min with 30 mM Alizarin Red S (ARS, A5533; Sigma-Aldrich) solution. Chondrogenic potential of ASC was evaluated on cell pellet cultures. About 200,000 ASC were centrifuged into 15 mL polystyrene conical tubes (BD Biosciences Falcon) and kept overnight in PCM. The culture medium was substituted the next day with DMEM, 0.1 μM dexamethasone, 100 ng/mL BMP6 (130-093-817, Miltenyi Biotec), 10 ng/mL transforming growth factor beta 1 (TGF-β1; 100-21C, Peprotech), 1% ITS+ Premix (354352; BD Biosciences), 50 ng/mL trisodium L-ascorbyl-2-phosphate (49752, Fluka; Sigma-Aldrich), and 40 ng/mL L-Proline (P5607; Sigma-Aldrich). Culture medium was changed daily and cell pellets were fixed after 21 days using 10% neutral buffered

formalin and embedded in paraffin. Five-μm microsections were rehydrated and stained with Alcian blue (88043, Richard Allan–Thermo-Fisher Scientific) for 30 min. The presence of lipid vesicles, ALP activity, calcium, and proteoglycans was documented using brightfield photomicroscopy.

Angiogenesis

Freshly isolated fat SVF or low-passage ASC were transferred into 0.1% gelatin-coated 8-well Lab-Tek™ chamber slides (Nunc™, Thermo-Fisher Scientific) at 10,000 cells/well and cultured for 14 days in Clonetics® EGM®-2 endothelial growth medium (CC-3156 supplemented with CC-4176, Lonza). Cells were fixed with PBS and 2% formaldehyde (15 min, ambient temperature) before performing immunofluorescent staining for von Willebrand factor (vWF), CD31, CD34, CD146, and alpha smooth muscle actin positive (α-SMA+).

Pleural effusion sample collection and preparation

All samples were waste materials from patients undergoing pleural drainage. De-identified samples were collected under an IRB-approved exemption (numbers 0503126 and 07090247, University of Pittsburgh IRB). MPEs ($n = 10$) were obtained from patients with documented metastatic adenocarcinoma of the breast. Heparinized samples (10 U/mL sodium heparin; Upjohn) were digested for 1 h with 0.4% collagenase type I (C0130; Sigma-Aldrich) and DNase type I (350 Kunitz units/mL, D5025; Sigma-Aldrich) solution in BioWhittaker® RPMI 1640 medium (12-167F; Lonza) and disaggregated through 100 mesh stainless steel screens. Viable cells were concentrated and separated from erythrocytes and debris on a Histopaque®-1077 Ficoll-Hypaque gradient.

MPE flow cytometry and cell sorting

Freshly isolated breast MPE cells were maintained on ice and stained for analytical flow cytometry and cell sorting experiments as previously described.[19,20] To minimize non-specific antibody binding, pelleted cells were incubated for 5 min with 5 μL neat decomplemented mouse serum (Sigma).[23] Analytical samples were simultaneously stained for surface markers with monoclonal mouse anti-human antibodies (20 min, 4°C, 2 μL each; CD44-PE [AbD Serotec, clone F10-44-2] or CD133/1-PE [Miltenyi Biotech, clone AC133], biotinylated CD90 [BD Biosciences, clone 5E10], CD14-PE-Cy5 [Beckman-Coulter, clone RMO52], CD33-PE-Cy5 [Beckman-Coulter, clone D3HL60.251], and CD235a-PE-Cy5 [BD Biosciences, clone GA-R2(HIR2)], CD117-PE-Cy7 [Beckman-Coulter, clone 104D2D1], CD133/2-APC [Miltenyi Biotech, clone 293C3], or CD326-APC [Miltenyi Biotech, clone HEA-124], and CD45-APC-Cy7 [BD Biosciences, clone 2D1]). Cells were washed in PBS, 4% calf serum and stained for 20 min on ice with ECD-conjugated streptavidin (IM3326, Beckman-Coulter). Samples were fixed with 2% methanol-free formaldehyde (Polysciences, Inc.) and then permeabilized with 0.1% saponin (Beckman-Coulter) and 0.5% human serum albumin in PBS for 10 min at room temperature. Pelleted permeabilized cells were incubated with 2 μL of anti-pan cytokeratin-FITC (IM2356; Beckman-Coulter) for 30 min. Cells were washed in 0.1% saponin and 0.5% human serum albumin in PBS, and resuspended to a final concentration of 25 million cells/mL in PBS with 7.7 μg/mL 4′,6-diamidino-2-

phenylindole (DAPI, D1306; Invitrogen) as described in the section Flow cytometric staining of ASC. Ten independent samples were analyzed. Flow cytometric results were summarized as arithmetic means ± SD and ± SEM, to convey both sample to sample variability (SD) and the precision of the mean values (SEM).[22]

Cell sorting was performed using a three-laser MoFlo high-speed cell sorter (Beckman-Coulter) equipped with a class I biosafety cabinet. Unfixed MPE cells were incubated for 5 min with 5 μL neat mouse serum and then simultaneously stained with monoclonal mouse anti-human antibodies (20 min, 4°C, 2 μL each; CD326-FITC [Miltenyi Biotec, clone HEA125], CD44-PE [AbD Serotec, clone F10-44-2], biotinylated CD90 [BD Biosciences, clone 5E10], CD14-PE-Cy5 [Beckman-Coulter, clone RMO52], CD33-PE-Cy5 [Beckman-Coulter, clone D3HL60.251], CD235a-PE-Cy5 [BD Biosciences, clone GA-R2(HIR2)], CD117-PE-Cy7 [Beckman-Coulter, clone 104D2D1], CD31-APC [R&D Systems, clone 9G11], and CD45-APC-Cy7 [BD Biosciences, clone 2D1]). Cells were washed in sterile PBS, incubated for 20 min on ice with ECD-conjugated streptavidin (IM3326; Beckman-Coulter), and finally resuspended in PBS, 2 mM ethylene-diaminetetraacetic acid (Sigma-Aldrich), and 0.5% BSA, supplemented with 2 μg/mL DAPI for exclusion of dead and apoptotic cells. Samples were continuously cooled to 4°C and four-way sorting was performed at 10,000–20,000 events/second (MoFlo sorter, Beckman-Coulter). Samples were collected into sterile polypropylene tubes containing 500 μL cold fetal calf serum (FCS, Atlanta Biologicals).

Coculture of CFSE-labeled stem cells and breast MPE cells

Freshly isolated breast MPE cells (5 individual samples) were admixed in equal numbers with low-passage CFSE-labeled ASC (isolated from 4 different patients, p1 to p4, 11 experiments) and plated into 0.1% gelatin-coated 8-well Lab-Tek™ chamber slides (Nunc™, Thermo-Fisher Scientific; 10,000 cells per well in quadruplicate). Cells were cultured in PCM and fixed in PBS and 2% methanol-free formaldehyde [15 min, room temperature] at 7 and 14 days. Tumor cell mitotic activity was estimated by counting the number of Ki67+ CFSE− cells per low power (10×objective) field. The entire wells (excluding edges) were counted. Results from replicate cultures were averaged and expressed as fold-increase over tumor alone control cultures. Statistics were performed on log-transformed counts, using Student's paired t-test (2-sided). The difference of experimental and control log values used in this test is the equivalent of a ratio (fold-difference) of arithmetic values.

Cytokine/chemokine bead array assay

ASC (4 patients) were matched (patient and passage) to samples used for *in vitro* coculture experiments as described in section Fat tissue collection, SVF isolation, and ASC preparation. Culture media were harvested 3 days after initial plating and snap-frozen for analysis of multiple secreted cytokine, chemokine, and growth factors. Fresh medium was used as a blank. Multiplexed analyte measurements were acquired using a dual-laser Luminex 100 Bio-Plex array system (Luminex Corporation) and processed at the Luminex Core Facility at the Hillman Cancer Center, Pittsburgh,

PA. All determinations were performed in duplicate using commercially available fluorophore-conjugated bead sets according to the manufacturer's instructions: the MILLI-PLEX® MAP (Millipore) High Sensitivity Human Cytokine kit with anti-human interleukin (IL)-1β (cat# HSIL-1B), IL-2 (cat# HSIL-2), IL-4 (cat# HSIL-4), IL-5 (cat# HSIL-5), IL-6 (cat# HSIL-6), IL-10 (cat# HSIL-10), IL-12p70 (cat# HSIL-12), IL-13 (cat# HSIL-13), and tumor necrosis factor alpha (cat# HSTNF-A) beads; the Human CVD panel 1 kit (cat# HCVD1-67AK) with anti-human soluble VCAM-1 (cat# HSP-SVCM1) and anti-human total plasminogen activator inhibitor-1 beads; the Cytokine/Chemokine kit (cat# MPXHCYTO-60K) with anti-human vascular endothelial growth factor (VEGF) beads (cat# MXHVEGF) and TGF-β1 single plex kit (cat# TGFB-64K-01). The Fluorokine MAP Multiplex Human Obesity Panel kit (cat# LOB000) was used in conjunction with anti-human adiponectin (cat# LOB 1065), C-reactive protein (cat# LOB1707), chemokine (C-C motif) ligand 2 (CCL2)/MCP-1 (cat# LUH279), complement factor D/adipsin (cat# LOB1824), leptin (cat# LUB398), and resistin beads (cat#LOB1359; all R&D Systems). CCL5 (regulated on activation, normal T expressed, and secreted [RANTES]) levels were measured using the RANTES Human Singleplex Bead Kit (Invitrogen, cat# LHC1031). The data were saved and evaluated as median fluorescence intensity using appropriate curve-fitting software (Bioplex software version 4.0, Bio-Rad Laboratories). The analyte concentration determined in the medium blank was subtracted from the measured concentration in the experimental samples.

NOD/SCID injections and animal care

Tumor xenograft studies. Experiments were performed under a protocol approved by our institutional animal care and use committee (protocol number 0909770). Female NOD.CB17-Prkdc[scid]/J (NOD/SCID, Cat. No. 001303) and NOD.Cg-Prkdc[scid] Il2rg[tm1Wjl]/SzJ (NSG, Cat. No. 005557) mice 6–8 weeks of age were purchased from The Jackson Laboratory, and housed five to a cage in a specific pathogen-free environment. Before injection of tumor cells, mice were anesthetized by methoxyflurane inhalation. For subcutaneous injection, a standard dose of 100 sorted cells was admixed with either irradiated unsorted MPE cells (10,000 rads from a [137]Ce source) or ASC. ASC were administered alone as a negative control. Cells were suspended in 25 µL ice-cold DMEM, 15% FBS, plus 25 µL Matrigel (356234; Becton Dickinson). Fifty µL of ice-cold cell suspension was injected subcutaneously into the mammary fat pads (4 injections/animal). Animals were examined twice weekly for behavioral changes and evidence of tumor. Mice were sacrificed 6 months postinjection. Harvested tissues were fixed in 10% neutral buffered formalin (Sigma). Paraffin embedding and sections (4–5 µm) were prepared at the McGowan Institute histology laboratory.

Immunostaining on paraffin-embedded tissues

Immunohistochemistry. Tissue microsections were deparaffinized in xylenes and rehydrated with a graded series of ethanol. Heat-mediated antigen retrieval was performed using Dako Target Retrieval Solution at pH9 (20 min, 125°C) in a Pascal pressure chamber (Dako). Endogenous peroxidase activity was quenched using the Dako Dual En-dogenous Enzyme-Blocking Reagent (10 min, ambient temperature). Tissue sections were washed twice in Dako Wash Buffer and then incubated for 1 h in blocking solution (PBS, 5% goat serum, 0.05% Tween 20) to reduce nonspecific antibody binding. Blocking solution was used for all subsequent antibody dilution. Primary antibodies were directly applied to tissue sections. Primary antibodies used were mouse anti-human cytokeratin (clone AE1/AE3, 1:100, and clone MNF116, 1:100, both Dako), CD90 (1:10, BD Biosciences 550402, clone 5E10), CD44 (1:50, Dako, M7082, clone DF1485, reported to bind to all CD44 isoforms[24]), Estrogen Receptor α (Ready to use, Dako, Cat. No. N1575), and Ki67 (Ready to use, Dako, cat. No. N1633, clone, MIB-1). Endogenous murine lymphomas were confirmed by the detection of murine CD45 (1:10, 550539, BD Biosciences, clone 30-F11). Primary antibodies were replaced by Universal Negative Control for Mouse Primary Antibodies (Ready to use, Dako cat. No. N1698) for negative controls. All primary antibodies and controls were incubated for 60 min at ambient temperature. Slides were washed 3 times in Dako Wash Buffer and then incubated with a horseradish peroxidase (HRP)-labeled polymer solution (EnVision™+ Dual Link System-HRP, K4061, Dako) for 30 min at room temperature. Slides were washed three times in Dako Wash Buffer and incubated with 3,3'-diaminobenzidine (DAB+) substrate-chromogen for 5 to 10 min. Tissue sections were washed twice in wash buffer before nuclear staining by hematoxylin (S3302, Dako, 5 min, ambient temperature). Slides were rinsed in deionized water and dehydrated in ethanol. Slides were finally immersed in xylenes and mounted in non-aqueous medium (Cytoseal™280, Richard-Allan Scientific). Specimens were photographed under brightfield microscopy (Nikon Labophot-2) using a digital camera (Spot Insight 2 Meg FW Color Mosaic model 18.2, Diagnostic Instruments, Inc.). Xenograft tumors were only scored as positive if they were human cytokeratin positive and evidenced histology consistent with epithelial carcinoma. The proportion of tumors in the different injection groups was compared using the χ^2 test (Fisher's exact test).

Immunofluorescence. For immunofluorescent staining, deparaffinization, rehydratation, endogenous peroxydase activity quenching, and blocking of nonspecific antibody binding were performed as above. Primary antibodies were incubated overnight at 4°C. Primary antibodies were mouse anti-human CD90 (1:10 [6.2µg/mL], 550402, BD Biosciences, clone 5E10) and CD44 (1:50 [7.6 µg/mL final concentration], M7082, Dako, clone DF1485), and rabbit anti-human chemokine (C-C motif) receptor 5 (CCR5) (1:200 [2.5 µg/mL final concentration], ab65850, Abcam) and MMP9 (1:50 [22 µg/mL final concentration], A0150, Dako). Universal Negative Control for Mouse Primary Antibodies (ready to use, N1698; Dako) and Universal Negative Control for Rabbit Primary Antibodies (ready to use, N1699; Dako) substituted primary antibodies for negative controls. Slides were washed three times in wash buffer and incubated for 1 h with a secondary biotinylated goat anti-mouse or goat anti-rabbit antibody solution (both 1:500; Dako). Slides were washed twice and incubated for 30 min with streptavidin-Cy3 (1:500; Sigma). After 3 washes, tissue sections were incubated for 1 h at ambient temperature with FITC-conjugated mouse anti-human pan-cytokeratin antibody

(clone C-11, 1:50; Abcam). Sections were washed twice and incubated for 5 min at ambient temperature with 7.15 μM DAPI solution for nuclear staining. Slides were washed twice in PBS and mounted using Prolong® Gold Antifade Reagent (P36934; Invitrogen).

Immunostaining of fixed Lab-Tek™ chamber slides

Chamber slide wells were detached before staining. Apart from deparaffinization, rehydration, and antigen retrieval steps, the same above-mentioned methodology was applied to stain fixed Lab-Tek™ chamber slides.

Immunohistochemistry. Double immunohistochemical staining was developed from the Dako Envison™ G|2 Doublestain System (Rabbit/Mouse, DAB+/Permanent Red, K5361; Dako). Fixed Lab-Tek™ chamber slides were washed twice in Dako Wash Buffer. Endogenous alkaline phosphatase and peroxidase activities were quenched using Dako Dual Endogenous Enzyme-Blocking Reagent (10 min, ambient temperature; S2003; Dako). Slides were washed twice and blocking solution was applied for 1 h at ambient temperature to eliminate nonspecific antibody binding. Biotinylated rabbit antifluorescein/Oregon Green® antibody (A-982, Invitrogen, 1:100, 10 μg/mL final concentration) was directly applied to the slides (1 h, ambient temperature). Slides were washed and incubated for 30 min at room temperature with streptavidin-HRP (ready to use, K0675; Dako). Alternatively antifluorescein antibody and streptavidin-HRP were substituted by mouse anti-human pan cytokeratin (1:100, 1.7 μg/mL final concentration, clone MNF116; Dako) and HRP-conjugated polymer (EnVision™+ Dual Link System-HRP, K4061; Dako), respectively. As negative controls, primary antibodies were replaced by Dako Universal Negative Control antibodies. Slides were washed three times in Dako Wash Buffer and incubated with DAB+ substrate-chromogen for 5 to 10 min. Tissue sections were washed twice in wash buffer and incubated with Dako Doublestain Block solution (5 min, ambient temperature). Slides were washed twice and mouse anti-human Ki67 (ready to use, N1633 Dako, clone MIB-1) was applied for 30 min (ambient temperature). After 2 washes, sections were incubated with a dextran polymer coupled with anti-rabbit and anti-mouse secondary antibodies (Rabbit/Mouse [LINK], Dako) for 20 min (ambient temperature). Specimens were rinsed twice and covered by alkaline phosphatase (AP)-labeled dextran polymer (Polymer/AP; Dako) for 20 min at ambient temperature. Slides were washed twice and incubated with Fast Red substrate-chromogen (Permanent Red; Dako) solution for 10 to 15 min at ambient temperature. Tissue sections were rinsed and immersed in hematoxylin (S3302, Dako, 5 min at ambient temperature) for nuclear staining. Slides were rinsed in deionized water, dehydrated in an increasing graded series of ethanol, immersed in xylenes, and mounted into nonaqueous medium (Cytoseal™280, 8311-4, Richard-Allan Scientific). Photomicrographs were acquired using a digital camera (Spot Insight 2 Meg FW Color Mosaic model 18.2; Diagnostic Instruments, Inc.) mounted on a brightfield microscope (Nikon Labophot-2).

Immunofluorescence. Fixed Lab-Tek™ chamber slides were washed twice in Dako Wash Buffer before blocking solution was applied for 1 h at ambient temperature. Slides

were then incubated with primary antibodies (mouse anti-human CD31 [1:50, 4 μg/mL final concentration, SC13537, Santa Cruz Biotechnology, clone 10G9], CD34 (1:50, 1 μg/mL final concentration, 347660, BD Biosciences, clone My10], and CD146 (1:100, 5 μg/mL final concentration, 550314, BD Biosciences, clone P1H12) for angiogenesis experiments and pan cytokeratin [1:100, Dako, clone MNF116] for coculture experiments) or Universal Negative Control for Mouse Primary Antibodies (Dako) for 1 h at ambient temperature. Slides were washed 3 times and incubated for 1 h with biotinylated goat anti-mouse antibody (1:500, 1.58 μg/mL final concentration, E0433; Dako). After 2 consecutive washes, specimens were incubated for 30 min with streptavidin-Cy3 (1:500, 2 μg/mL final concentration, S6402; Sigma). For double immunostaining, tissue sections were washed three times and incubated for 1 h at ambient temperature with sheep anti-human FITC-conjugated vWF (1:100, V2700-01C; US Biological) or mouse anti-human FITC-conjugated α-SMA (1:100, F3777, Sigma-Aldrich, clone 1A4) antibodies. Sections were washed twice and nuclear staining was achieved by a 5-min incubation at ambient temperature with DAPI (7.15 μM; Invitrogen). After 2 washes in PBS, slides were mounted using Prolong® Gold Antifade Reagent.

Results

Effect of ASC coculture on proliferation of breast cancer clinical isolates

Breast MPE cells were admixed in equal numbers (5000 cells for each population) with CFSE-labeled low-passage ASC (11 experiments) and cultured in Lab-Tek™ chamber slides. One week after culture initiation, proliferating MPE cells were identified as clusters of unlabeled cells in the midst of a confluent layer of CFSE+/cytokeratin− ASC (Fig. 1). Cytokeratin+/CFSE− epithelioid MPE cells assumed a compact organization when growing among ASC. Proliferation of MPE cells was assessed by Ki67 immunocytochemical staining. Ki67+/CFSE− proliferating MPE cells were counted at low magnification in quadruplicate wells. We evaluated the effect of feeder cells as the fold-change in Ki67+ mitotic tumor cells. The number of proliferating MPE cells increased after the addition of ASC (Table 1, 5.1 ± 0.68, mean ± SEM, paired Student's t-test, $p < 0.0005$).

Characterization of CD90+ small resting and large active tumor cells in breast cancer pleural effusions

Despite the absence of vessels and varying amounts of normal and dysplastic breast tissue found in primary breast tumors, MPE cells are heterogeneous. Analytical flow cytometry was performed as previously described on 10 individual clinical isolates, first eliminating sources of artifact, then identifying populations of interest by eliminating hematopoietic and mesothelial[25] cells, and finally measuring outcomes on these populations.[20,26] After removal of debris, cell clusters, and apoptotic events, nonhematopoietic cells were negatively selected based on CD45 expression. A lineage gate (CD14, CD33, and CD235a) was incorporated into the analysis of the majority of the samples (Fig. 2a). The resulting nonhematopoietic, nonmesothelial (nonheme) fraction represented 0.03% to 44.7% of all acquired debris-free
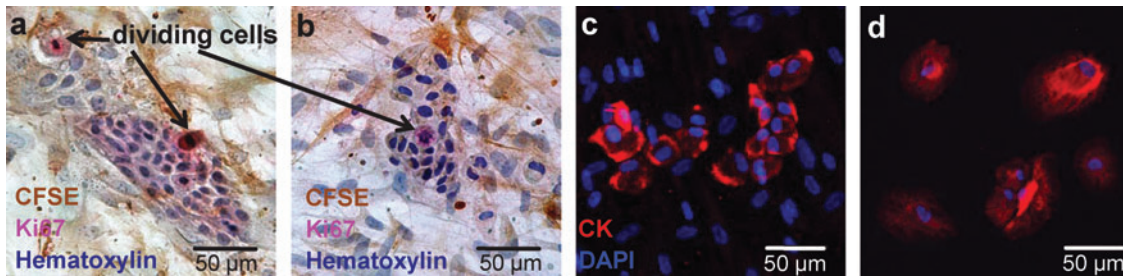
FIG. 1. Freshly isolated unsorted breast malignant pleural effusion (MPE) cells were cocultured for 1 **(a, c)** or 2 **(b)** weeks in Labtek culture chambers with low passage carboxyfluorescein succinimidyl ester (CFSE)-labeled adipose-derived stem cells (ASCs). Cells were fixed with 2% formaldehyde and stained for immunohistochemistry or immunofluorescence. MPE cells were cultured alone as control **(d)**. ASC were observed using an antifluorescein antibody and revealed by 3,3′-diamino-benzidine staining (brown, **a**, **b**). Nests of CFSE− tumor cells were surrounded by CFSE+ ASC **(a, b)**. MPE cells were further identified as cytokeratin+ using immunofluorescence **(c, d,** red**)**. Tumor cell mitotic activity was estimated by counting the number of Ki67+ mitotic figures, excluding CFSE+ feeder cells **(a, b,** pink**)**. Color images available online at www .liebertonline.com/ten.

events (15.25 ± 16.28%, mean ± SD). CD90+ cells represented 13.9% ± 17.5% of nonheme cells. The small (low light scatter) CD90+ subpopulation was selected according to a region adjusted to the light scatter profile of resting CD14−/ CD33−/CD45+/CD235a− lymphocytes (Fig. 2, top right, color-evented red). The low light scatter CD90+ nonheme population was limited to 9.62 ± 13.07% of CD90+/CD45−/ heme lineage-negative cells. Both small and large (high light scatter) CD90+ subpopulations, as well as CD90− nonheme cells were further analyzed for their DNA content and for expression of epithelial markers (cytokeratin and epithelial cell adhesion molecule [EpCAM]) and stem/progenitor cell markers (CD44, CD133, and CD117) (Fig. 2; Table 2). Small CD90+/CD45− cells were mostly quiescent, in contrast to their larger-sized counterpart in which the DNA content of 11% of cells was >2N (Table 1). In contrast, CD90−/CD45− cells presented an intermediate heterogeneous phenotype. While the great majority of large CD90+ cells coexpressed the epithelial marker cytokeratin, less than half of the small population was cytokeratin positive. Strikingly, EpCAM was poorly expressed by small CD90+ cells. EpCAM expression was higher among CD90− cells compared with CD90+/CD45− cells. Small and large CD90+ populations also differed with respect to CD44 expression.

While most large CD90+ cells coexpressed CD44, CD44 was detected on only a third of small CD90+ cells. Although restricted to a small proportion of nonhematopoietic cells, CD133 expression was virtually absent on small CD90+/ CD45− cells, compared with large CD90+ and CD90− nonheme cells. CD117 expression was uniformly low on all populations (1.74 ± 0.77% of CD45− cells). Figure 2 illustrates a representative example of pleural effusion cells where small CD90+ cells exhibit a resting phenotype (DAPI linear histogram) associated with low levels of cytokeratin and intermediate levels of CD44 expression. In contrast, large CD90+ cells uniformly coexpress cytokeratin and CD44, and have a large proportion of cycling/aneuploid cells.

Effect of ASC on *in vivo tumorigenesis* of small and large CD90+CD31−CD45− tumor cells

Despite its utility, the *in vitro* coculture model system suffers from several limitations: (1) it requires relatively large numbers of tumor cells (5000/well), precluding analysis of rare sorted tumor cell populations; (2) culture time was limited to 14 days, after which feeder cells become confluent. The tumor xenograft model overcomes these limitations because (1) it requires few tumor cells per injection site, (2)

TABLE 1. AUGMENTATION OF *IN VITRO* TUMOR GROWTH BY ADIPOSE-DERIVED STEM CELLS

	Ki67+ Cells/low power field (fold-change compared to no ASC)					
Feeders↓ MPE→	*PE16*	*PE49*	*PE28*	*PE31*	*PE83*	*Mean*
Ø	9.75 (1)	1.75 (1)	0.75 (1)	0.25 (1)	1 (1)	2.7 (1)
FatSC01-30-07 p4	30.5 (3.13)	13.5 (7.71)				22.0 (5.42)
FatSC03-20-07 p2			4.5 (6.0)	1.75 (7.0)	5.25 (5.25)	3.83 (6.08)
FatSC05-24-07 p2			4.5 (6.0)	1.5 (6.0)	2.75 (2.75)	2.92 (4.92)
FatSC10-20-08 p1			1 (1.33)	2 (8.0)	2.75 (2.75)	1.92 (4.03)
Mean	30.5 (3.13)	13.5 (7.71)	3.33 (4.44)	1.75 (7.0)	3.58 (3.58)	7.67 (5.11[a])

MPE from five independent samples were cocultured for 1 week with ASC from 4 independent sources. Cultures were plated in quadruplicate. The mean number of proliferating MPE cells per low power field (10×objective) and the fold change in proliferating cells after coculture are tabulated.

[a]Statistical significance ($p = 0.0005$) determined by Student's 2-tailed *t*-test (null hypothesis: fold-change = 1). PE numbers (column headings) represent independent clinical isolates.

ASCs, adipose-derived stem cells; MPE, metastatic pleural effusion.
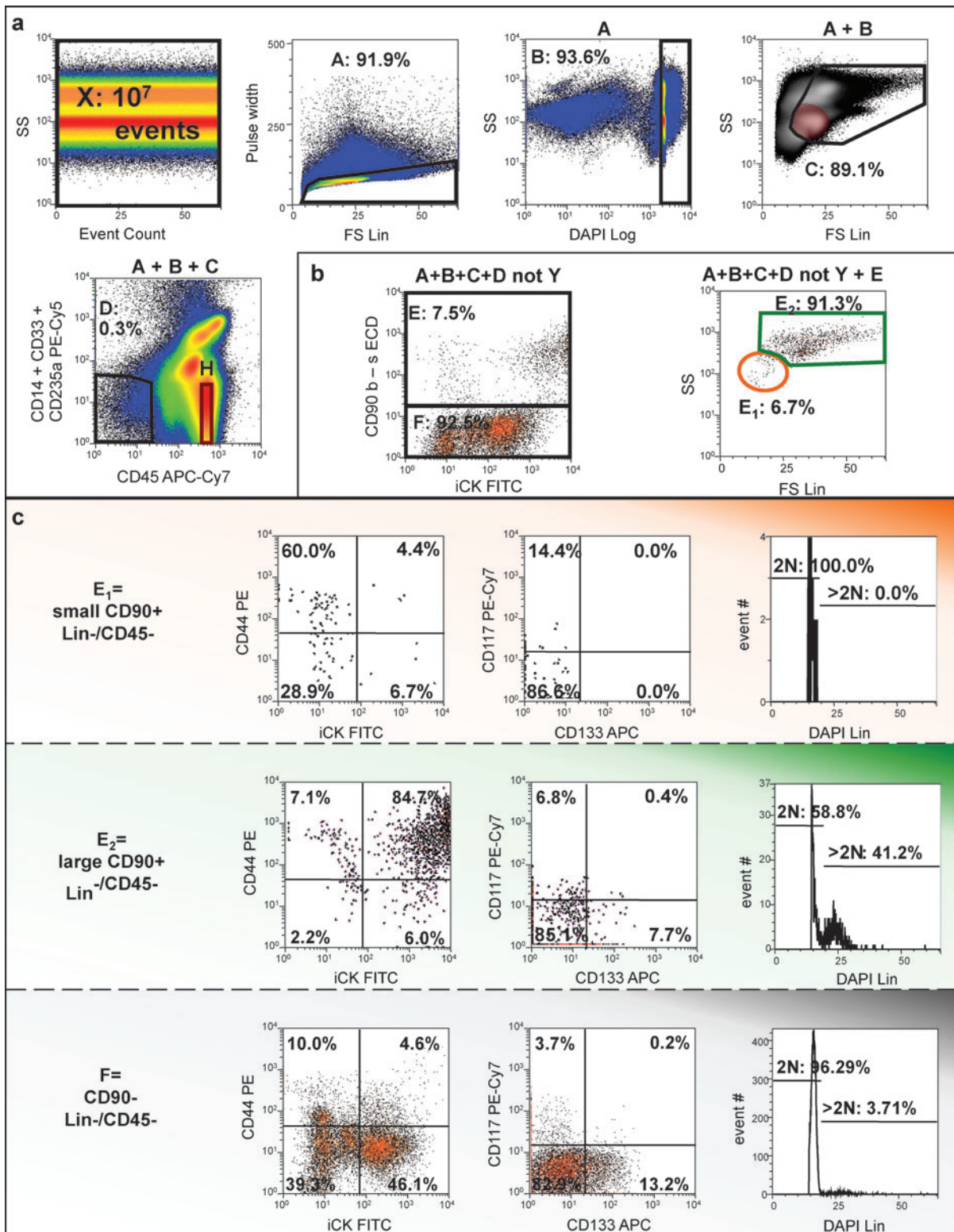
FIG. 2. Detection and characterization of CD90+ breast cancer cells in a pleural effusion. **(a)** Elimination of sources of artifact. A representative sample (10 million events) is presented. After confirming the absence of fluidic disturbances (side scatter vs. event count), cell clusters were eliminated based on pulse analysis (region A), before selecting nucleated DAPI+ events with DNA content ≥2N (region B) and removing subcellular particles and early apoptotic cells. Region C was adjusted based on the localization of CD14−CD33−CD235a−CD45+ resting lymphocytes (H, color evented red in the SS vs. FS panel). Nonhematopoietic cells and cell-binding antibody nonspecifically were selected and removed from further analysis using CD45 and a lineage cocktail. **(b)** Identification of large, active (high light scatter) and small resting (low light scatter) CD90+ breast cancer cells. Nonhematopoietic CD90+ cells were selected (region E) and subdivided into two distinct populations based on their light scatter profile (regions E1 and E2). **(c)** Both small and large CD90+ subpopulations and CD90− cells were further analyzed for expression of cytokeratin, CD44, CD133, CD117, and DNA profile (DAPI). Color images available online at www.liebertonline.com/ten.

TABLE 2. FLOW CYTOMETRIC CHARACTERIZATION OF SMALL CD90+, LARGE CD90+ AND CD90−
NONHEMATOPOIETIC BREAST CANCER CELLS ISOLATED FROM PLEURAL EFFUSIONS

			Nonheme CD45−/Lin−								
			CD90+						CD90−		
			High light scatter CD90+			Low light scatter CD90+					
			Mean (%)	SD (%)	SEM (%)	Mean (%)	SD (%)	SEM (%)	Mean (%)	SD (%)	SEM (%)
Cell cycle	G0/G1	DNA = 2N	89.44	13.75	5.20	97.88	1.61	0.61	94.12	3.96	1.50
	Cycling or aneuploid	DNA > 2N	10.56			2.12			5.88		
Expressing	Epithelial markers	Pan cytokeratin	88.59	15.13	4.78	44.38	36.25	11.46	40.97	37.56	11.88
		Epithelial cell adhesion molecule	10.83	20.89	7.38	1.79	3.11	1.10	23.49	33.00	11.67
	Stem cell markers	CD44	84.68	9.26	4.14	30.71	23.62	10.56	40.87	42.11	18.83
		CD117	1.68	2.33	0.78	2.06	4.80	1.60	1.69	2.35	0.78
		CD133	4.86	5.18	1.83	0.63	1.25	0.44	4.11	5.18	1.83

SD, standard deviation; SEM, standard error of the mean.

animals can be held for months until palpable tumors develop, and (3) the murine mammary fat is an orthotopic growth site that may provide niche effects absent *in vitro*. To assess the effects of ASC on subpopulations of tumor cells (in particular, rare resting CD90+ cells), we adapted a xenograft model detailed previously[18,19] in which injection of tumorigenic CD90+ cells in limiting number (as low as 100 cells) gives rise to tumors in a proportion of immunodeficient animals by 6 months after injection. Nonhematopoietic (CD45−), nonmesothelial (CD14−), nonendothelial (CD31−) breast MPE cells from two patients were sorted into three distinct fractions: (1) small, resting (low light scatter) CD90+; (2) large, metabolically active (high light scatter) CD90+, and (3) CD90−. Together, these fractions comprised all of the potentially tumorigenic populations in the MPE. Sorted MPE subpopulations were injected (100 cells per injection) into the mammary fat pads, either alone or coinjected with feeder cells (4 sites of injection for each animal and 40 injections for each sorted population). Feeder cells were either ASC (2 subjects) or irradiated unsorted MPE cells (10,000 feeder cells per injection and 20 injections for feeder cell only controls). For the second experiment, we changed from NOD/SCID to IL2rγ null mice because of the marked incidence of spontaneous murine lymphomas in NOD-SCID mice (25 of 70 mice, one of which required early sacrifice at day 93). Lymphomas were confirmed at necropsy by the detection of murine CD45.1 expression by immunohistochemistry (not shown). Tumors at the injection sites were followed by palpation and confirmed as human epithelial tumors by immunohistochemistry at necropsy (Fig. 3a, b, q). All injection-site tumors were of human origin as confirmed by expression of a set of human-specific reagents (cytokeratin clone MNF116, CD44, and CD90) (Fig. 3p–s). All cytokeratin+ cells expressed cell surface CD44. CD90 expression was restricted to a small proportion of cytokeratin+ tumor cells, as well as to isolated capillaries and stromal cells within the tumor, indicating the human origin of these nonmalignant tissues. All tumors exhibited expression of CCR5 and MMP9, markers of tumor invasion and metastasis. CCR5 expression was detected on isolated nests of cytokeratin+ tumor cells, whereas MMP9 was present on the majority of tumor cells (Fig. 3j–o). Consistent with the phenotype of the original tumors, all tumor xenografts uniformly expressed estrogen receptor alpha. Despite the slow growth kinetics of the tumors, a significant proportion of tumor cells were actively in cycle as determined by Ki67 expression, suggesting a continuous process of proliferation and apoptosis (Fig. 3t).

Large, active CD90+/CD31−/CD45− MPE cells were not tumorigenic when injected alone at 100 cells per site. The coinjection of 10,000 ASC, but not an equal number of heavily irradiated (100 Gray) unsorted tumor cells, greatly enhanced tumorigenicity of this population (42.5% of injection sites, χ^2 test $p = 0.00017$), demonstrating the dramatic effect of ASC on the proliferation of large, active CD90+ cells (Table 3; Fig. 3). In contrast, injection of 100 small resting CD90+/CD31−/CD45− MPE cells in the absence of feeder cells gave rise to tumors in a small proportion of animals, and was not affected by coinjection of either ASC or irradiated tumor. Finally, as previously reported[18] CD90−/CD31−/CD45− nonhematopoietic cells were not tumorigenic at 100 cells per injection site, with or without feeder cells.

ASC resemble bone marrow-derived MSCs in phenotype and potentiality

ASC were selected by plastic adherence of the adipose stromal vascular fraction (SVF). After a short *in vitro* expansion (1 to 3 passages), cells were trypsinized and analyzed by flow cytometry (Fig. 4). While low-passage ASC lack expression of the endothelial marker CD31, a variable, but limited proportion (7.61 ± 8.69%, mean ± SD) of residual CD45+ hematopoietic cells could still be detected. Similar to BM-MSCs,[27] ASC homogenously expressed the mesenchymal markers CD105, CD73, CD90, and CD44. In addition to these classical mesenchymal markers, persistent expression of both CD146 and CD34 was observed. We have previously shown that these markers specify two distinct stromal/vascular populations, adipose pericytes and supra-adventitial adipose stromal cells (SA-ASC), respectively, both of which are adipogenic.[21]

TABLE 3. QUANTIFICATION OF TUMORIGENESIS OF SORTED BREAST CANCER METASTATIC PLEURAL EFFUSION CELLS WITH OR WITHOUT ADJUNCTION OF FEEDER POPULATIONS

Feeder cells → Tumor cells ↓	Experiment 1 (positive sites/total sites)		Experiment 2 (positive sites/total sites)		Summary (%)	
	10,000 ASC	10,000 irradiated CD90−CD31−CD45− tumor cells	10,000 ASC	10,000 irradiated CD90−CD31−CD45− tumor cells	10,000 ASC	10,000 irradiated CD90−CD31−CD45− tumor cells
100 high scatter CD90+CD31−CD45− tumor cells	9/20	0/20	8/20	0/20	42.5% $p < 0.0005$[a]	0%
100 low scatter CD90+CD31−CD45− tumor cells	3/20	5/20	1/20	1/20	10% N.S.[a]	15%
100 CD90−CD31−CD45− tumor cells	0/20	0/20	0/20	0/20	0% N.S.[a]	0%
Ø	0/20	0/20	ND	ND	0% N.S.[a]	0%

Experiment 1 utilized NOD-SCID mice; experiment 2 used IL2rγ-null mice. χ^2 comparison between ASC and irradiated tumor feeder cells.
IL, interleukin.
[a]p-value by χ^2.

To confirm the BM-MSC-like properties of low-passage ASC, we investigated the differentiation potential of ASC toward mesenchymal lineages. After a short *in vitro* expansion, ASC were separated for subsequent culture with addition of either adipogenic, osteogenic, or chondrogenic factors. When cultured under adipogenic conditions, ASC differentiated efficiently into mature adipocytes with enlarged lipid vesicles (Fig. 4Ba). To assay for their chondrogenic potential, ASC were pelleted and cultured using a chondrogenic medium. Paraffin sections of cultured cell pellets revealed the presence of proteoglycans, a marker of chondrogenic differentiation. Finally, ASC showed alkaline phosphatase activity and produced calcium, as detected by Alizarin red, when differentiated toward the osteogenic lineage. (Fig. 4Bc,d) Thus, ASC fulfill all three criteria for the definition of MSCs[27]: adherence, immunophenotype, and differentiation toward mesenchymal lineages.

Because freshly isolated fat SVF cells and low-passage ASCs are candidate cell populations for regenerative therapy, we investigated whether they can also participate in or promote angiogenesis. Freshly isolated fat SVF cells and first-passage ASC were cultured *in vitro* in the endothelial growth medium (EGM2) (Fig. 4B). Networks of endothelial tubules coexpressing the endothelial markers CD31 and vWF formed over a confluent layer of adherent adipose-derived fibroblasts (Fig. 4Be). Consistent with vascular endothelium, CD34 and CD146 expression was also detected on these networks, which were surrounded in some areas by α-SMA+ fibroblasts.

ASC have a unique secretome

To explore potential mechanisms by which ASC could promote the growth of primary breast cancer cells in culture, we measured the levels of a battery of cytokines, chemokines, and growth factors secreted by low-passage ASC using the Luminex® multiplexed immunoassay (Table 4). As reported for BM-MSC,[28] ASC secreted CCL2, IL-6, plasminogen activator inhibitor-1, VEGF, and sVCAM, as well as TGF-β1, and failed to secrete detectable levels of interleukins IL-1b, IL-2, IL-4, IL-5, IL-10, IL-12, and IL-13 or the chemokine CCL5 (RANTES) or adiponectin, CRP, resistin, or tumor necrosis factor alpha. ASC uniquely secreted adipsin and leptin, suggesting that despite their immunophenotypic similarity to BM-MSC, they are skewed toward a fat-related repertoire of secreted proteins that could account for their differing-abilities to promote the growth of breast cancer tumor cells from clinical isolates.

Discussion

Regenerative therapy after cancer surgery

Breast cancer surgery can be disfiguring. The advent of tissue engineering presents the opportunity for more natural and stable breast reconstruction postmastectomy. A major difficulty facing the use of ASC-augmented autologous fat grafts is that the same elements that favor graft stability, namely, angiogenesis and growth factor production,[9–11] may also promote survival of residual tumor.[29] There is a growing body of literature demonstrating that ASC, or closely related MSC, can promote tumor growth.[30–32] These experiments were performed exclusively using rapidly growing cell lines that fail to model the natural history of breast cancer, where
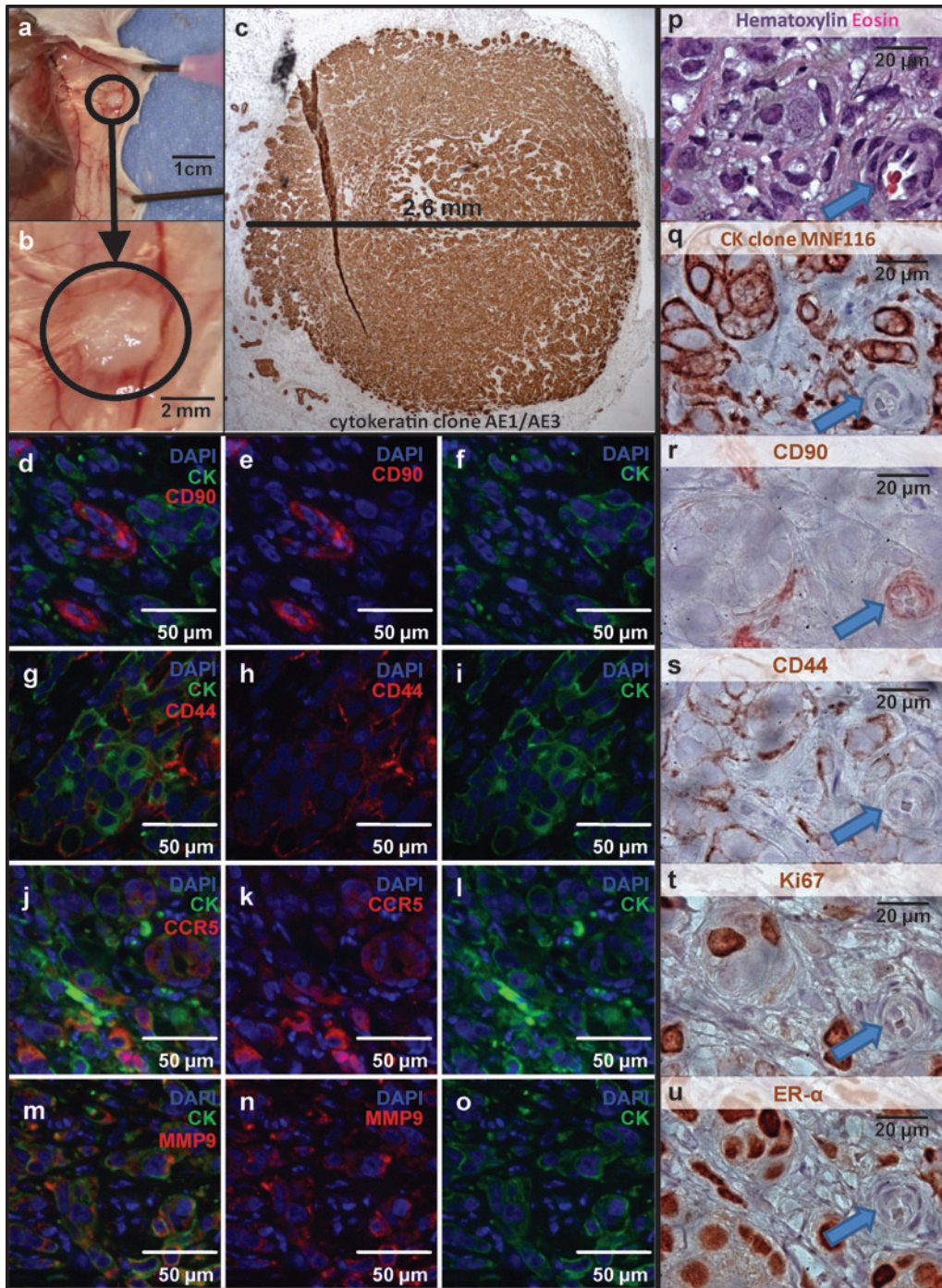
FIG. 3. *In vivo* tumorigenesis mouse xenograft model. Breast MPE cells were sorted into three distinct nonhematopoietic nonendothelial (CD31− Lin− CD45−) fractions based on their CD90 expression and light scatter profiles (small CD90+ vs. large CD90+ vs. CD90− cells) and were injected (100 cells per injection) into the mammary fat pads of NOD-SCID or NOD/Shi− scid interleukin-2rγ null mice (4 injection sites/animal). Sorted MPE cells were either injected alone or coinjected with either 10,000 ASC or with heavily irradiated MPE cells. Animals were sacrificed up to 6 months postinjection. Representative photographs of successful tumorigenesis are shown. Upon tissue harvesting, the presence of tumors at the site of injection was documented (**a,** and enlargement **b**). All injected sites were analyzed by immunohistochemistry and tumorigenesis was confirmed by detection of a cellular mass expressing the epithelial marker cytokeratin (**c, q,** brown). Both cross species-specific (AE1/AE3) and human-specific (MNF116) antibody clones were routinely used. Tumors were further characterized by immunofluorescence (**d–o,** 40×objective) and immunohistochemistry (**p–u,** 100×objective). Human CD90 expression was observed on small groups of cells distributed throughout the tumor and was largely restricted to nonepithelial cells (**d–f**) and small vessels (**r,** arrow). In contrast, CD44 was expressed at the membrane of all cytokeratin+ tumor cells (**g–i**). Tumors expressed both chemokine (C-C motif) receptor 5 (CCR5) and MMP9, markers of tumor invasion and metastasis. CCR5+ cells were detected as isolated groups of cells, whereas MMP9 was homogenously expressed throughout the tumor. A representative tumor was documented at higher magnification through serial immunostaining (**p–u**). The majority of tumor epithelial cells expressed estrogen receptor alpha (**u**). Despite the slow kinetics of tumor growth, a significant number of tumor cells were actively proliferating as shown by expression of Ki67 (**t**).
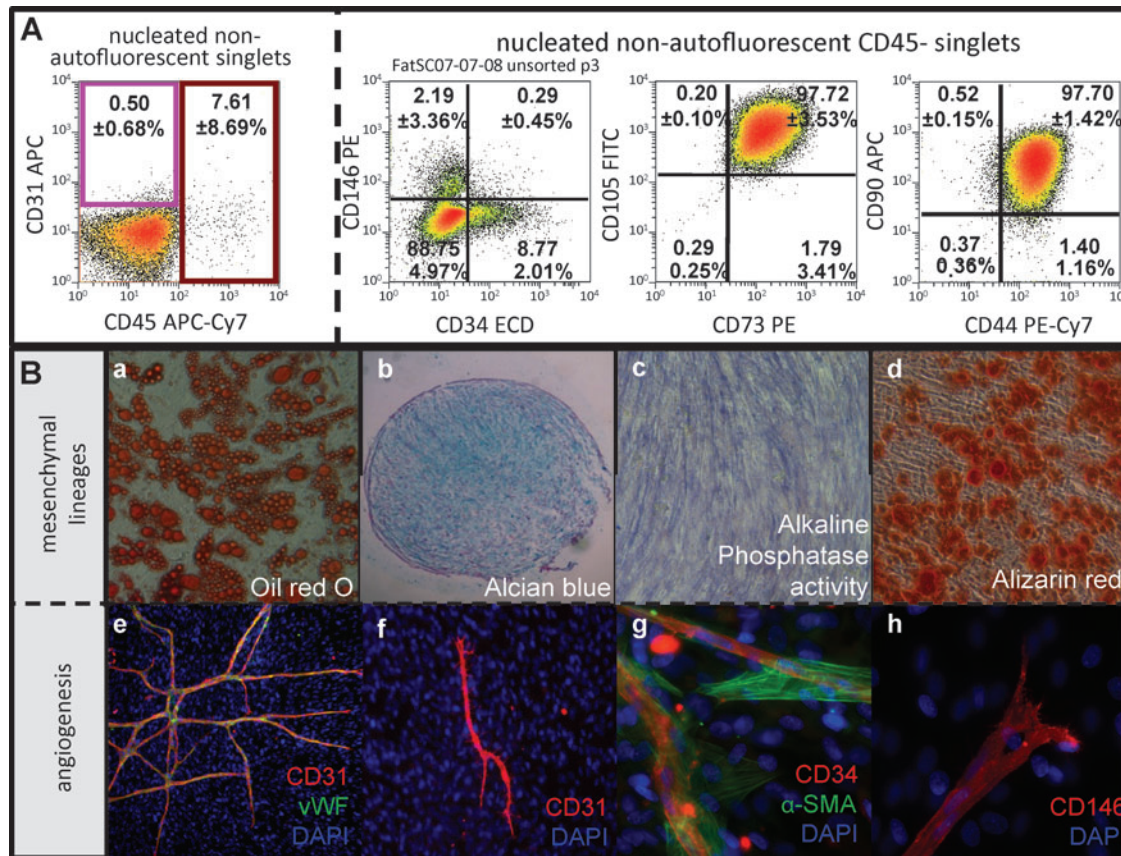
FIG. 4. Immunophenotype and functional characterization of mesenchymal stem cell-like ASC. Immunophenotype: ASC were briefly expanded (passage 1 to passage 3) and analyzed by flow cytometry. A representative sample is shown including quantitative results from five independent samples (mean ± standard deviation; box **A**). ASC do not express the mature endothelial marker CD31. Persistence of CD45+ cells (primarily macrophages) during early passages is inconsistent, as reflected in the large standard deviation. ASC strongly and homogeneously express the mesenchymal markers CD105, CD73, CD90, and CD44. Small subpopulations of CD146+ and CD34+ cells can still be detected during early passages. These markers are associated with distinct perivascular fat populations (adipose pericytes and SA-ASC respectively), from which ASC are derived. ASC are able to differentiate *in vitro* toward mesenchymal lineages. **(a)** Oil red O staining (red) reveals the presence of lipid vesicles in differentiated ASC under adipogenic culture conditions (box **B**). **(b)** The presence of proteoglycans after *in vitro* differentiation reflects the chondrogenic potential of ASC as shown by Alcian blue staining (blue). **(c, d)** ASC osteogenic differentiation is assessed by alkaline phosphatase activity staining (blue, **c**) and calcium staining (alizarin red staining, red). **(e–h)** Freshly isolated stromal vascular cells (stromal vascular fraction) exhibit strong angiogenic potential *in vitro* (coexpression of mature endothelial markers CD31, red; von Willebrand factor [vWF], green); **(e)** ASC retain a limited *in vitro* angiogenic potential after short expansion (tubule formation, CD31 expression in red). **(f–h)** In addition to CD31 and vWF, other endothelial/perivascular marker (CD34, CD146, and alpha smooth muscle actin [α-SMA]) expressing cells are observed in the endothelial tubules. Five independent experiments were performed.

residual tumor may remain dormant,[17,33] only to reactivate years after apparently successful therapy. The goal of the present investigation was to develop a model more relevant to regenerative therapy after cancer surgery, using clinical isolates rather than cell lines. Unlike breast cancer cell lines, metastatic pleural effusions are heterogeneous, are difficult to establish in culture, and require months to form detectable tumors in immunodeficient mice.[18,19]

MPE ASC coculture

The advantages of using MPE as a tumor cell source are the lack of extreme *in vitro* selection encountered in cell lines and the relative scarcity of nonmalignant epithelial cells[19] compared to primary tumor. Metastatic pleural effusions

also capture the phenotypic heterogeneity encountered in clinical isolates. Despite this heterogeneity, MPE consistently express high levels of metastasis-related proteins, such as ezrin and claudin-4, compared to primary tumors.[34] Culture of MPE cells in the presence of low-passage ASC unequivocally promoted the growth of MPE cells (5.1-fold increase, $p = 0.0005$) (Fig. 1; Table 1). After 1 week of coculture, nests of dividing epithelial cells were detected interspersed among a monolayer of ASC. Such nests were not observed when MPE were cultured alone.

Tumor xenografts

Resting hematopoietic stem cells have been associated with a low light scatter profile.[35] We applied this principle to

Table 4. Cytokines, Chemokines, and Growth
Factors Produced by Adipose-Derived Stem Cells

Cytokines/chemokines/growth factors	Mean ± SEM (ng/mL)
Adiponectin	<0.34
Adipsin (CFD)	74.0 ± 2.5
CCL2 (MCP1)	1.6 ± 0.2
CCL5 (RANTES)	<0.02
C-reactive protein (CRP)	<0.03
IL-1b	<0.0001
IL-2	<0.0001
IL-4	<0.0001
IL-5	<0.0001
IL-6	1.1 ± 0.6
IL-10	<0.0001
IL-12	<0.0001
IL-13	<0.0001
Leptin	7.0 ± 2.0
Plasminogen activator inhibitor-1 (serpine2)	>50
Resistin	<0.04
Transforming growth factor beta 1	1.2 ± 0.04
Tumor necrosis factor alpha	<0.0001
sVCAM (CD106)	0.5 ± 0.3
Vascular endothelial growth factor	0.2 ± 0.06

Supernatants of low-passage ASC were harvested 3 days after plating when cultures were ∼80% confluent and assayed using the Luminex multiplexed bead assay. Results of four independent ASC preparations are shown (mean ± SEM). These are the identical preparations used for coculture experiments.

CCL, chemokine (C-C motif) ligand; RANTES, regulated on activation, normal T expressed and secreted.

nonheme CD90+ MPE cells and identified two cell populations based on forward and side light scatter characteristics. We previously demonstrated that both large, active CD90+ MPE cells and small resting CD90+ MPE cells are tumorigenic in immunodeficient mice.[19] However, when given in limiting doses (40–100 cells per injection site), only small resting CD90+ MPE cells produced tumors.[18,19] In the present study we examined the effect of coinjection of low-passage ASC on tumorigenicity of low dose (100 cells/site) small/resting and large/active CD90+ cells, and CD90− cells (Table 3). Together, these three fractions accounted for all nonhematopoietic, nonendothelial cells in the MPE. In agreement with our previous data, only the small resting CD90+ cells were tumorigenic when low numbers of MPE cells were injected without supporting ASC.[19] Coinjection of ASC did not increase the tumorigenic frequency of small resting CD90+ cells. In contrast, large, active CD90+ cells, which were not tumorigenic alone at 100 cells/injection, caused tumors in 42.5% of injection sites when coadministered with 10,000 ASC. CD90− MPE cells did not generate tumors with or without ASC.

What is the biology underlying these findings and how can these results be related to regenerative therapy? From the standpoint of ASC, the ability to support the growth of large, active CD90+ tumor cells is consistent with experiments performed with rapidly proliferating cell lines[30] and can be explained by ASC-mediated production of mesenchymal growth factors VEGF, TGF-β, and IL-6, plus the adipose-specific hormone leptin and the serine protease adipsin. Leptin has been shown to support the growth of breast cancer

cells.[36–38] The role of adipsin is not known but could assist in tumor invasiveness. In our xenograft experiments, it is likely that ASC not only provided growth factors, but gave rise to stroma and vessels as well. Through the use of human-specific anti-CD90 antibody we demonstrated the participation of human cells in tumor vascularization. The human component of these chimeric vessels may have originated from either ASC or tumor cells, or both. That ASC mediated a differential effect on active and resting CD90+ MPE may be explained by the low number of cells injected and the different requirements of these tumor fractions for survival. We speculate that unlike active CD90+ high light scatter cells, resting CD90+ low light scatter cells are more autonomous and do not immediately require growth factor or angiogenic support of ASC for survival and eventual tumorigenesis. The growth of resting CD90+ low light scatter MPE cells is sufficiently slow and they are sufficiently resistant to apoptosis that they can recruit vascularization and supportive stroma on their own during the months-long process of generation of palpable tumors. We further speculate that these resting tumor cells are responsible for cancer dormancy and late recurrence in the natural host.

Conclusions

The applicability of results to clinical practice should be viewed with caution. Delay recently published a large series of cases in which 880 breast reconstructions were performed using autologous fat, but not ASC. Some of the participants included patients undergoing nipple-areola reconstruction after mastectomy. In this cohort, which had a maximal follow-up of 10 years, there was no detectable increase in risk of local recurrence or new cancer development.[4] The present results, which indicate that ASC augment the growth of active but not resting breast cancer cells, suggest that reconstructive therapy utilizing ASC-augmented whole fat should be postponed until there is no evidence of active disease. If our xenograft results can be extrapolated, they also suggest that the use of ASC to promote breast tissue regeneration should not affect the status of dormant residual cancer cells.

Authors' Contributions

Drs. Vera and Albert Donnenberg contributed equally to this article, sharing responsibility for experimental design, data interpretation, and article preparation. Ludovic Zimmerlin, graduate student in the Donnenberg laboratory, performed all *in vitro* experiments and immunohistostaining and contributed significantly to data analysis and article preparation. Dr. Basse supervised all animal experiments. Dr. Rubin provided all adipose tissue samples and was instrumental in focusing this article on the clinical problem of reconstruction after mastectomy. Dr. Landreneau provided pleural effusions and anonymized clinical data for the breast cancer patients.

Acknowledgments

Disclosure Statement

None of the authors have competing interests that would have influenced the preparation of this article.

References

1. Neuber, G.A. Fettransplantation. Chir Kongr Verhandl Deutsche Gesellschaft für Chirurgie 22, 66, 1893.
2. Czerny, V. Plastischer Ersatz der Brustdruse durch ein Lipom. Chir Kong Verhandl 2, 216, 1895.
3. ASPRS. Report on autologous fat transplantation. ASPRS Ad-Hoc Committee on New Procedures, September 30, 1987. Plast Surg Nurs 7, 140, 1987.
4. Delay, E., Garson, S., Tousson, G., and Sinna R. Fat injection to the breast: technique, results, and indications based on 880 procedures over 10 years. Aesthet Surg J 29, 360, 2009.
5. Peer, L.A. Loss of Weight and Volume in Human Fat Grafts: With Postulation of A "Cell Survival Theory." Plast Reconstr Surg 5, 217, 1950.
6. Calabria, R., and Hills, B. Fat grafting: fact or fiction? Aesthet Surg J 25, 55, 2005.
7. Billings, E., Jr., and May, J.W., Jr. Historical review and present status of free fat graft autotransplantation in plastic and reconstructive surgery. Plast Reconstr Surg 83, 368, 1989.
8. Nguyen, A., Pasyk, K.A., Bouvier, T.N., Hassett, C.A., and Argenta, L.C. Comparative study of survival of autologous adipose tissue taken and transplanted by different techniques. Plast Reconstr Surg 85, 378; discussion 87, 1990.
9. Moseley, T.A., Zhu, M., and Hedrick, M.H. Adipose-derived stem and progenitor cells as fillers in plastic and reconstructive surgery. Plast Reconstr Surg 118, 121S, 2006.
10. Yoshimura, K., Sato, K., Aoi, N., Kurita, M., Hirohi, T., and Harii, K. Cell-assisted lipotransfer for cosmetic breast augmentation: supportive use of adipose-derived stem/stromal cells. Aesthetic Plast Surg 32, 48; discussion 6, 2008.
11. Zhu, M., Zhou, Z., Chen, Y., Schreiber, R., Ransom, J.T., Fraser, J.K., et al. Supplementation of fat grafts with adipose-derived regenerative cells improves long-term graft retention. Ann Plast Surg 64, 222, 2010.
12. Miranville, A., Heeschen, C., Sengenes, C., Curat, C.A., Busse, R., and Bouloumie, A. Improvement of postnatal neovascularization by human adipose tissue-derived stem cells. Circulation 110, 349, 2004.
13. Planat-Benard, V., Silvestre, J.S., Cousin, B., Andre, M., Nibbelink, M., Tamarat, R., et al. Plasticity of human adipose lineage cells toward endothelial cells: physiological and therapeutic perspectives. Circulation 109, 656, 2004.
14. Gronthos, S., Franklin, D.M., Leddy, H.A., Robey, P.G., Storms, R.W., and Gimble, J.M. Surface protein characterization of human adipose tissue-derived stromal cells. J Cell Physiol 189, 54, 2001.
15. Zuk, P.A., Zhu, M., Mizuno, H., Huang, J., Futrell, J.W., Katz, A.J., et al. Multilineage cells from human adipose tissue: implications for cell-based therapies. Tissue Eng 7, 211, 2001.
16. Strem, B.M., Hicok, K.C., Zhu, M., Wulur, I., Alfonso, Z., Schreiber, R.E., et al. Multipotential differentiation of adipose tissue-derived stem cells. Keio J Med 54, 132, 2005.
17. Brewster, A.M., Hortobagyi, G.N., Broglio, K.R., Kau, S.W., Santa-Maria, C.A., Arun, B., et al. Residual risk of breast cancer recurrence 5 years after adjuvant therapy. J Natl Cancer Inst 100, 1179, 2008.
18. Donnenberg, V.S., Donnenberg, A.D., Zimmerlin, L., Landreneau, R.J., Bhargava, R., Wetzel, R.A., et al. Localization of CD44 and CD90 positive cells to the invasive front of breast tumors. Clin Cytometry 2010 [Epub ahead of print].
19. Donnenberg, V.S., Luketich, J.D., Landreneau, R.J., DeLoia, J.A., Basse, P., and Donnenberg, A.D. Tumorigenic epithelial stem cells and their normal counterparts. Ernst Schering Found Symp Proc 5, 245, 2006.
20. Zimmerlin, L., Donnenberg, V.S., and Donnenberg, A.D. Rare event detection and analysis in flow cytometry: bone marrow mesenchymal stem cells, breast cancer stem/progenitor cells in malignant effusions, and pericytes in disaggregated adipose tissue. In: Hawley, T.S., and Hawley, R.G., eds. Flow Cytometry Protocols. Third Edition. New York: Humana Press, 2011 (In press).
21. Zimmerlin, L., Donnenberg, V.S., Pfeifer, M.E., Meyer, E.M., Peault, B., Rubin, J.P., et al. Stromal vascular progenitors in adult human adipose tissue. Cytometry A 77A, 22, 2010.
22. Donnenberg, A.D. Statistics of immunological testing. In: O'Gorman, M.R., and Donnenberg, A.D., eds. Handbook of Human Immunology. Second Edition. Boca Raton: CRC Press Taylor and Francis, 2008. p. 29.
23. Donnenberg, A.D., and Donnenberg, V.S. Rare-event analysis in flow cytometry. Clin Lab Med 27, 627, viii, 2007.
24. Horny, H.P., Menke, D.M., and Kaiserling, E. Neoplastic human tissue mast cells express the adhesion molecule CD44/HCAM. Virchows Arch 429, 91, 1996.
25. Ross, J.A., Ansell, I., Hjelle, J.T., Miller-Hjelle, M.A., and Dobbie, J.W. Phenotypic and functional characterisation of human mesothelial cells. Tissue Antigens 55, 2, 2000.
26. Donnenberg, V.S., Landreneau, R.J., and Donnenberg, A.D. Tumorigenic stem and progenitor cells: implications for the therapeutic index of anti-cancer agents. J Control Release 122, 385, 2007.
27. Dominici, M., Le Blanc, K., Mueller, I., Slaper-Cortenbach, I., Marini, F., Krause, D., et al. Minimal criteria for defining multipotent mesenchymal stromal cells. The International Society for Cellular Therapy position statement. Cytotherapy 8, 315, 2006.
28. da Silva Meirelles, L., Fontes, A.M., Covas, D.T., and Caplan, A.I. Mechanisms involved in the therapeutic properties of mesenchymal stem cells. Cytokine Growth Factor Rev 20, 419, 2010.
29. Almog, N., Ma, L., Raychowdhury, R., Schwager, C., Erber, R., Short, S., et al. Transcriptional switch of dormant tumors to fast-growing angiogenic phenotype. Cancer Res 69, 836, 2009.
30. Muehlberg, F.L., Song, Y.H., Krohn, A., Pinilla, S.P., Droll, L.H., Leng, X., et al. Tissue-resident stem cells promote breast cancer growth and metastasis. Carcinogenesis 30, 589, 2009.
31. Pinilla, S., Alt, E., Abdul Khalek, F.J., Jotzu, C., Muehlberg, F., Beckmann, C., et al. Tissue resident stem cells produce CCL5 under the influence of cancer cells and thereby

promote breast cancer cell invasion. Cancer Lett **284,** 80, 2009.

32. Karnoub, A.E., Dash, A.B., Vo, A.P., Sullivan, A., Brooks, M.W., Bell, G.W., *et al.* Mesenchymal stem cells within tumour stroma promote breast cancer metastasis. Nature **449,** 557, 2007.

33. Naumov, G.N., MacDonald, I.C., Chambers, A.F., and Groom, A.C. Solitary cancer cells as a possible source of tumour dormancy? Semin Cancer Biol **11,** 271, 2001.

34. Konstantinovsky, S., Smith, Y., Zilber, S., Tuft Stavnes, H., Becker, A.M., Nesland, J.M., *et al.* Breast carcinoma cells in primary tumors and effusions have different gene array profiles. J Oncol **2010,** 969084, 2009.

35. Grogan, W.M., Haar, J.L., Scott, R.B., and Collins, J.M. Applications of light scatter to separation of stem cells. Blood Cells **6,** 625, 1980.

36. Vona-Davis, L., and Rose, D.P. Adipokines as endocrine, paracrine, and autocrine factors in breast cancer risk and progression. Endocr Relat Cancer **14,** 189, 2007.

37. Goodwin, P.J., Ennis, M., Fantus, I.G., Pritchard, K.I., Trudeau, M.E., Koo, J., *et al.* Is leptin a mediator of adverse prognostic effects of obesity in breast cancer? J Clin Oncol **23,** 6037, 2005.

38. Iyengar, P., Combs, T.P., Shah, S.J., Gouon-Evans, V., Pollard, J.W., Albanese, C., *et al.* Adipocyte-secreted factors synergistically promote mammary tumorigenesis through induction of anti-apoptotic transcriptional programs and proto-oncogene stabilization. Oncogene **22,** 6408, 2003.

Address correspondence to:
Vera S. Donnenberg, Ph.D., F.C.P.
University of Pittsburgh Cancer Institute
5117 Centre Ave.
Suite 2.42b, Hillman Cancer Center Research Pavilion
Pittsburgh, PA 15213

E-mail: donnenbergvs@upmc.edu